Theoretical UV Circular Dichroism of Cyclo(L-Proline-L-Proline)

Kristine L. Carlson, Stephen L. Lowe, Mark R. Hoffmann, and Kathryn A. Thomasson*

Department of Chemistry, University of North Dakota, Grand Forks, North Dakota 58202-9024

Received: June 1, 2005; In Final Form: November 23, 2005

MP2, DFT, and molecular mechanics (AMBER, CVFF, and CFF91) geometry optimizations were performed on the cyclic dipeptide cyclo(L-Pro-L-Pro) starting from crystal structure data. Three stable conformations were identified as energy minima by all methods, but assignment of relative energy varied between the methods. The π—π* transition feature of the UV circular dichroic (CD) spectrum was predicted for each minimized structure using the classical physics method of the dipole interaction model. The model was sensitive to the different conformations. The UV-CD predictions were compared individually and as a Boltzmann-weighted composite with published experimental CD spectra [Bowman, R. L.; Kellerman, M.; Johnson, W. C., Jr. *Biopolymers* **1983**, *22*, 1045]. For all structures, the original parameters of Applequist [Applequist, J. *J. Chem. Phys.* **1979**, *71*, 4324] with a bandwidth of 3000 cm^{-1} most accurately replicated experiment, except for the CFF91 structures, which matched experiment best with a bandwidth of 4000 cm^{-1}. The inclusion of solvent by a continuum model did not significantly alter the minimized geometries obtained by molecular or quantum mechanics, but it did have an effect on the relative predicted energies of CFF91 and B3LYP conformations. The overall effect of solvent inclusion was negligible when Boltzmann-weighted spectra were considered. Gas-phase CFF91 structures were also reasonably good for prediction of CD spectra, and when water was included via a continuum model for energy calculations, the weighting scheme resembled that of the higher-level weightings. The CD calculated using the MP2/6-311G** structures and energies for weighting were most descriptive of the 180 nm negative band in the experimental CD, but red-shifted the location of the 205 nm band. DFT structures were comparably, though not identically, as descriptive of the first π—π* band, and did a better job with placement of the second (positive) π—π* band. DFT calculations were less sensitive to basis set effect than the MP2 calculations, with 6-31G* results in close agreement with 6-311G**. The results suggest that it is possible to use geometries obtained from a variety of different methods (molecular mechanical or quantum mechanical) with the classical physics dipole interaction model to qualitatively reproduce the UV CD of model amides.

Introduction

The dipole interaction model, a classical physics method, has proven qualitatively successful for predicting the far-UV circular dichroism (CD) of several aliphatic piperazine-2,5-diones (cyclic dipeptides) when structures are optimized by quantum mechanical calculations; therefore, the effects of molecular geometry on CD spectral calculations via classical physics can be reliably assessed.[1] Herein, the somewhat flexible cyclic proline dipeptide cyclo(L-Pro-L-Pro) (5*H*,10*H*-dipyrrolo[1,2-a:1′,2′−d]pyrazine-5,10-dione) is treated. Three characteristics of this aliphatic piperazine-2,5-dione make it a particularly challenging molecule to examine theoretically and computationally. First, it contains proline: Proline is of interest because its amide bonds in vivo may be either cis or trans, and proline is commonly found in protein turn structures and tends to disrupt α-helices.[2,3] Second, cyclo(-L-Pro-L-Pro) possesses considerable restriction on accessible backbone conformations because of the side chain rings of proline and the cyclic backbone. Third, despite the conformational restrictions, the proline side chain itself is flexible, resulting in a semiflexible cyclic dipeptide. Experimental and theoretical studies by other groups[4,5] have shown the existence of three conformations in solution; however, only one crystal structure has been reported.[6] Previously, the combination of classical CD predictions combined with quantum mechanical geometries demonstrated the existence of a higher-energy conformation of cyclo(-L-Pro)$_3$ that could not be observed via crystallography or NMR.[2] Thus, the distribution of the cyclo(-L-Pro-L-Pro) conformations in solution may also be resolved through examination of its theoretical circular dichroic spectrum.

Theoretical Investigation of Molecular Structure. Modeling chemical systems complements traditional "wet lab" investigations. Rapid processes that are not resolvable by usual spectroscopic methods, structural ensembles that do not resolve clearly, and mechanisms of reactions all may be understood in greater depth when mathematical models of the system behavior are used. When modeling chemical systems, one may choose to use classical physics-based molecular mechanics (MM) or quantum physics-based quantum mechanics (QM) methods. MM treatment offers the advantage of rapid computation time owing to simplifying approximations of bonding behavior corrected by experimental parameter fitting. QM treatment can be extremely precise, but is mathematically complex, and the computational expense of QM methods scales as third- (e.g., DFT) or higher-order polynomials with size. Thus, large biological systems are inaccessible to highly accurate methods, especially when calculating spectral properties such as vibrational frequencies.

Verification of model system accuracy is accomplished by comparison to experimental data. One form of experiment with

* To whom correspondence should be addressed. E-mail: kthomasson@chem.und.edu. Phone: 701-777-3199. Fax: 701-777-2331.

10.1021/jp052924k CCC: $33.50 © 2006 American Chemical Society
Published on Web 01/12/2006

which to compare is circular dichroism (CD). CD is one of the general molecular and ensemble-level spectroscopic techniques, accessible in the solvated environment, that provides insight into structural properties such as secondary structure content of proteins.[7,8] CD measures the difference in absorption of left and right circularly polarized light in the absence of a magnetic field. As electrons in the molecule absorb light, the transition of electrons into local excited states induce dipole moments within the molecule. These induced dipole moments interact with one another electrically and magnetically. The amide groups in proteins possess characteristic $\pi-\pi^*$ transitions (180−210 nm, ∼140 nm) and $n-\pi^*$ transitions (220 nm) whose locations and intensities indicate secondary structural features of the peptide.[9]

Circular dichroism (CD) has several advantages over other methods for determining structure. First, CD does not require high-quality crystals such as those necessary for X-ray crystallography. Second, CD works well with small concentrations (orders of magnitude less than NMR experiments). Third, CD works for macromolecules that are too large to be investigated by NMR.[10] A crystal structure is a static picture that provides limited insights into the dynamic aspects of structure crucial to function. CD is often used to monitor dynamic conformational changes in solution such as folding/unfolding processes and conformational changes upon protein−protein and protein−ligand binding.[11−13]

There are several methods to predict CD spectra for a molecule with knowledge of its structure. Quantum mechanics allows for direct solution of the dipole and rotational strength, although this is computationally infeasible for large systems. One approximation to handle larger molecules divides the molecule into a number of separate model chromophores and treats those chromophores quantum mechanically. Coupled with solution of the Schrödinger equation for isolated model chromophores over ground and excited states, this splitting yields the method of Tinoco[14] and the matrix method.[15−17] While accurate, this method is computationally expensive and subject to the limitations of all QM treatments for size accessibility; to meet that restriction, not all side chains are included in the calculations.[18] Thus, the effects of nonchromophoric portions of the molecule on the chromophores are not accounted for in this method, even though they have been shown to be quite important in treatment of proline-containing peptides.[19] Incorporating a small fraction of the side chain has been shown to improve the matrix method predictions for poly-L-proline II, but results suggest that a larger fraction of the nonchromophoric part may need to be included.[20]

Classical physics models may also be used to calculate CD. The time savings in relation to the QM models are enormous; while calculating one simple cyclic dipeptide structure's CD spectra ab initio using a QM method may take days, the same structure's CD may be predicted in mere seconds using a classical model. The dipole interaction model[21−25] is one such classical physics-based method for predicting the CD of peptides and proteins. This model includes all atoms explicitly, except the amide group, as points having nondispersive polarizability; the amide group is treated as a single point possessing dispersive polarizability. In the dipole interaction model, the sum over all dispersive oscillators (light-absorbing units, where there are q dispersive oscillators) of the interaction of the rotational strength (R_k) at each wavenumber ($\bar{\nu}$) describes the CD ($\Delta\epsilon$) spectrum. The rotational strength of each segment of the molecule is obtained by dividing the molecule into atoms with isotropic and anisotropic polarizability. The relationship between R_k and the measured $\Delta\epsilon$ is given by eq 1 for the classical dipole interaction model, assuming a Lorentzian band shape[22,24,26−28]

$$\Delta\epsilon = \frac{32\pi^3\bar{\nu}^3 N_A \Gamma}{6909n} \sum_{k=1}^{q} \left\{ \frac{R_k}{(\bar{\nu}_k^{\,2} - \bar{\nu}^2)^2 + \Gamma^2\bar{\nu}^2} \right\} \qquad (1)$$

N_A is Avogadro's number, Γ is the half-peak bandwidth, n is the number of peptide residues, and ν_k is the normal-mode wavenumber. This model has been parametrized for the $\pi-\pi^*$ transition of amides in peptides and proteins including the original parameters,[21,29] general peptide structures (G parameters), α−helical structures (H parameters), and poly-L-Pro-II structures (J parameters).[25,29,30]

The dipole interaction model has proven successful for a variety of applications, including the prediction of CD spectra for β-sheets,[31] β-turns,[32,33] α-helices,[21,34] β-peptides,[35−37] and a variety of cyclic peptides,[2,32,38−41] and is the only classical method published to obtain the correct $\pi-\pi^*$ spectrum for poly-L-proline II[19,42] and for collagen.[43] The model has previously proven insightful for cyclo(L-Pro-L-Pro), but this treatment did not take into account the flexibility of the proline side chain nor did it allow for variations in the C−C bond lengths.[38] The dipole interaction model has also proven successful on whole proteins including α-spectrin, tropomyosin,[34] and lactate dehydrogenase.[44] These earlier studies suggest that comparison of theoretical CD for a geometrically optimized structure to the experimental CD reasonably assesses the validity of calculated structures. Furthermore, by comparing the predicted CD to experiment, the dipole interaction model has provided clear evidence of the importance of ensembles in predicting CD. For example, for cyclo(L-Pro)3, the experimental spectrum could only be reproduced when an ensemble of two distinctly different structures were included in the calculation, even though the higher-energy structure only contributed approximately 20%.[2]

Herein, the dipole interaction model is tested with cyclo(L-Pro-L-Pro) geometries predicted via a variety of molecular modeling techniques including molecular mechanics and the MP2 and DFT methods of quantum mechanics, which account for electron correlation. The following questions are addressed: (1) Which method of structural optimization is best for use with the dipole interaction model for cyclo(L-Pro-L-Pro)? (2) Which of the dipole interaction parameters are best suited for use for cyclo(L-Pro-L-Pro), and do they coincide with the optimal parameters for other piperzaine-2,5-diones studied previously?[1] (3) How quantitatively do the dipole interaction model's predictions compare with experimental values? (4) Does the dipole interaction model recognize poor geometries (i.e., is it a good tool for evaluating molecular geometries)? (5) Can the dipole interaction model handle multiple conformations in a shallow potential energy surface?

Methods.

Geometric Optimization. The crystal structure[45] of cyclo(L-Pro-L-Pro) was obtained through the Cambridge Structural Database[20] via the ConQuest software (code CLPRPR).[46] The structure was imported into InsightII (2000) (Accelyrs, San Diego, CA), where the molecular energy was geometrically minimized using the AMBER,[47,48] CVFF,[49] and CFF91[50] force fields with a quasi-Newton Raphson algorithm. The crystal geometry of the cyclic dipeptide was modified by manual alteration of the dihedral angles to achieve inverted ring geometries. Geometric optimization of the structures by energy minimization using quantum mechanical calculations was carried

out in *Gaussian 98*[51] and *Gaussian 03*.[52] Restricted Hartree−Fock (RHF), a hybrid DFT Becke3-LYP (B3LYP) functional method,[53−55] and two pure DFT methods were explored: Becke-VWN (BVWN)[53,55,56] and Becke−Lee−Yang−Parr (BLYP).[53,54,56] Second-order Moller−Plesset perturbation theory (MP2)[57,58] was used to investigate the structure of the cyclic dipeptide while taking into account explicitly correlational effects. Frequency calculations were carried out at the same level of theory as the geometry optimizations. A series of Pople-style double- and triple-split valence basis sets were used in the optimizations at each level: 6-31G[59−64] and 6-311G.[65] Single d polarization functions were added to the 6-31G[62] and 6-311G[65] basis sets (denoted 6-31G* and 6-311G*), and both d and p polarization functions were used with the 6-311G basis set (6-311G**). The 6-31G* calculations used pure d functions (i.e., five functions per set), whereas the triple split calculations used all six Cartesian d functions. The GDIIS algorithm was used with very tight geometric optimization convergence criteria (maximum force 2×10^{-6} mdyn/Å). A grid size setting of "ultrafine" (90 radial shells, 590 angular points per shell) was used for computing integrals over atomic basis functions. For each of these optimizations, SCF gradient convergence was set to 1.0×10^{-10}.

Solvent effects (water) were considered using a dielectric constant in the MM optimizations. The PCM[66−69] model was used to investigate the role of solvent (water, as in the experiments herein used for comparison[4]) on structure and subsequent CD spectra with B3LYP/6-31G* and MP2/6-311G** calculations. The PCM-B3LYP geometric optimizations were started from previously obtained gas-phase structures. PCM-MP2 geometric optimization was performed on the PCM-B3LYP/6-31G* optimized geometries. These calculations were performed on SGI Fuel workstations, except for the MP2 calculations, which were performed on a multiprocessor Origin300 server.

Structural Comparison. Molecular geometries obtained by both quantum mechanics and molecular mechanics were analyzed with ChemBats3D Pro (CambridgeSoft, Cambridge, MA), and PDB files were generated for each structure using the same software. Values for bond lengths, bond angles, and dihedral angles were compared for each minimization with crystal structure values. Standard assignments of dihedral angles are used; for the diketopiperazine ring, they are defined as ψ_n ($C_k'-N_n-C_n^{\alpha}-C_n'$), ϕ_n ($N_n-C_n^{\alpha}-C_n'-N_k$), and ω_n ($C_n^{\alpha}-C_n'-N_k-C_k^{\alpha}$), where the subscript n refers to the residue number in the sequence of the dipeptide and the subscript k indicates the next residue.

CD Calculation. Cartesian coordinate files generated from the PDB files exported from InsightII were used to calculate the $\pi-\pi^*$ transition of each optimization's CD spectrum by the dipole interaction model.[21,24,28,70] This was accomplished through direct use of coordinates for the nonchromophoric portions of each molecule, while the amide (the chromophore) was reduced to a single point and the Eulerian angles between the first chromophore and each successive chromophore were calculated. The original parameters,[24,26,71] general peptide parameters, α-helical system parameters, and poly-L-Pro-II parameters [25,30] were all used to predict the $\pi-\pi^*$ feature of the CD spectrum for each molecule between 140 and 260 nm with a step size of 0.5 nm. For each of the general peptide, helical system, and poly-L-Pro-II parameter CD calculations, the location of the amide chromophore was given three possibilities: centered on the N−C′ bond (o), shifted 0.1 Å toward the C′ atom on the N−C′ bond (x), and shifted 0.1 Å in the NCO′ plane above the N−C′ bond (y). For the original parameter set, only the first location was used because that is what has historically worked best with this model.[24,26] The CD spectrum for each structure was calculated between 150 and 250 nm with a 0.5 nm interval and half-peak bandwidths of 3000, 4000, and 5000 cm^{-1}. Boltzmann-weighted CDs were determined by using the total energies at 298 K, i.e., including vibrational and rotational contributions as computed in the *Gaussian 98* or *Gaussian 03* frequency analysis or from the molecular mechanics force field minimization, and also using the distribution of 70% platter, 15% boat, and 15% chair suggested by Bour et al.[5]

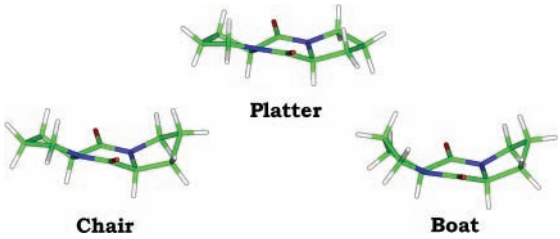

Figure 1. Three-dimensional representation of the minimum-energy conformations of cyclo(L-Pro-L-Pro). Structures shown were obtained through MP2 geometric optimization using the 6-311G** basis set.

Analysis of CD Calculations. OriginPro 7.5 (OriginLab Corporation, Northampton, MA) was used to locate the CD spectra peaks and determine half-peak bandwidths, which represent the integrated rotational strength of the combined oscillators. This was accomplished with the peak-fitting module by setting the baseline to $\Delta\epsilon = 0$ and allowing the software to locate peaks automatically. No data preconditioning was used, and all features were fit to Lorentzian bands. A default value of 100 iterations was set for fitting at a 95% confidence value. Published experimental CD spectra were compared with the calculated values for cyclo(L-Pro-L-Pro).

Results

Molecular Conformation. Three minimum-energy conformations were found for cyclo(L-Pro-L-Pro) (Figure 1), consistent with the results of Bour et al. and experimental observations.[5] For clarity of discussion, we call them the "platter", "chair", and "boat" conformations, consistent with organic nomenclature. The platter conformation is that identified by X-ray crystallography.[6] The calculated ϕ, ψ, and ω angles indicate that the diketopiperazine ring remains mostly unchanged; ω, however, may vary by as much as 5° and ψ by as much as 10° among the three conformations obtained using a single geometric optimization method (Supporting Information). The diketopiperazine ring conformation differences are most marked in the MP2 optimized structures and virtually absent in the CVFF and AMBER minimizations. Using basis sets larger than 6-31G* had a very negligible effect on the geometries of each conformation. Structural variation was greater between individual conformations generated by different methods (RHF, MP2, etc.) than between the same conformation generated via any particular method using differing basis sets (6-31G*, 6-311G*, etc.) (Figure 2).

Inclusion of solvent effects through use of a dielectric constant in the MM calculations led to reduction in strain on the ϕ dihedral angles (Figure 2). This relaxation was most noticeable in the CFF91 structures. The large ω values for these structures (−14° to −18°), however, are questionable. Even with the relaxation induced by inclusion of implicit solvent, the ϕ angles of the CFF91 and CVFF platter conformation structures remain

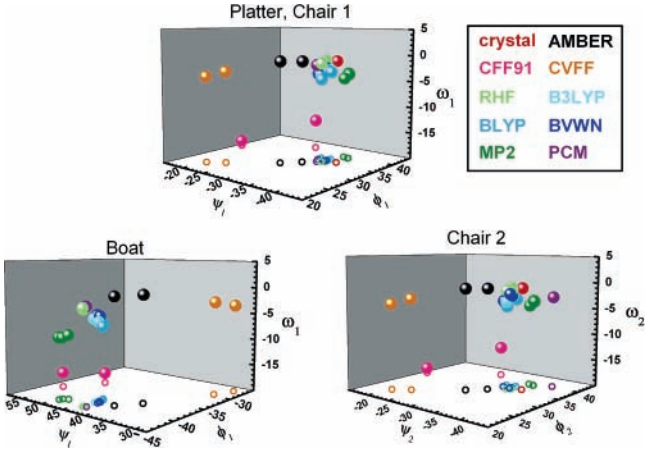

Figure 2. Dihedral angles of cyclo(L-Pro-L-Pro) in the three conformations. "Platter" and "Boat" denote the dihedral angles of the platter and boat conformations, respectively. The platter and boat conformations have C_2 symmetry, so both residues in each dipeptide have identical dihedral angles. "Chair 1" denotes the dihedral angles of one proline unit, and "Chair 2" denotes the dihedral angles of the other proline unit in the chair conformation. The spheres locate ϕ, ψ, and ω three-dimensionally, and the open circles represent the two-dimensional shadow on the ϕ/ψ wall.

considerably smaller than those of the other structures (27° and 23°, respectively) and outside the range of expected "good" ϕ values.[72] The structures calculated using PCM with B3LYP and MP2 were identical to one another. The ω angles flattened out to very near 0° in these calculations, and most of the reduction in energy obtained by PCM can probably be attributed to stabilization of the planar amide groups.

Calculated Energies. The calculated relative energies of the structures of cyclo(L-Pro-L-Pro) are listed in Table 1. Every method used, except RHF, identified the platter conformation as the minimum-energy structure, but the energy differences between the structures varied by method. All DFT methods indicate a fairly equal population between the conformations. The Boltzmann distribution of the ensemble at room temperature is each conformation comprising approximately $^1/_3$ of the population, but there is a slight preference for the platter conformation. The MP2 calculations, however, show a significant basis set effect on relative energies of the conformations, as do the RHF calculations (despite the geometries remaining unaltered by variation of basis set). Using a large basis set (6-311G*), the MP2-calculated relative energies suggest a similar conformational distribution to those determined by the DFT relative energies. The gas-phase MM force field energies show a distinct difference between the conformational energies and favor the platter (crystal-like) structure significantly. The energy distribution obtained using CFF91 minimizations including solvent (water) implicitly resemble the quantum mechanics distributions; the estimated energy differences between the conformations are considerably less than those obtained by all other MM calculations. When the implicit solvent model was applied with MP2 geometries and energies, the population distribution remained unchanged from the gas-phase calculations. The use of implicit solvent to model the effects of water on energy and geometry in the B3LYP calculations led to increased chair and boat conformation populations.

CD Spectra. Applequist's original parameters gave the best agreement with experiment for every structure calculated for all descriptors of the bands: location of the peak, sign, and half-peak bandwidth (Figure 3). This is in agreement with previous results for other aliphatic piperazine-2,5-diones.[1] The general

TABLE 1: Internal Energies at 298 K and Boltzmann Distribution Values for Each Conformation

	internal energy (kcal/mol)			difference from platter		Boltzmann distribution		
	$E_{platter}$	E_{chair}	E_{boat}	ΔE_{chair}	ΔE_{boat}	platter	chair	boat
				MM − Water				
AMBER	18.31	20.60	22.59	2.28	4.28	0.98	0.02	0.00
CFF91	12.77	13.40	13.07	0.64	0.30	0.51	0.18	0.31
CVFF	40.19	43.36	46.37	3.17	6.18	1.00	0.00	0.00
				MM − Gas				
AMBER	56.13	58.42	60.48	2.29	4.36	0.98	0.02	0.00
CFF91	49.05	50.58	51.05	1.53	1.99	0.87	0.07	0.07
CVFF	80.76	84.04	87.17	3.29	6.42	0.99	0.00	0.00
				RHF				
6-31G*	168.58	168.64	168.70	0.05	0.12	0.37	0.33	0.30
6-311G*	167.70	166.36	167.81	−1.31	0.13	0.09	0.84	0.07
6-311G**	166.88	165.66	167.01	−1.22	0.13	0.10	0.82	0.08
				B3LYP				
6-31G*	157.70	157.81	157.87	0.04	0.09	0.36	0.34	0.31
6-311G*	157.09	157.13	157.18	0.04	0.09	0.35	0.33	0.33
6-311G**	156.56	156.60	156.65	0.04	0.09	0.37	0.32	0.32
				BLYP				
6-31G*	153.05	153.11	153.18	0.06	0.13	0.37	0.33	0.30
6-311G*	152.47	152.52	152.59	0.05	0.12	0.35	0.32	0.32
6-311G**	152.01	152.07	152.14	0.06	0.13	0.38	0.31	0.31
				BVWN				
6-31G*	154.60	154.63	154.63	0.03	0.04	0.35	0.33	0.33
6-311G*	154.04	154.09	154.07	0.05	0.03	0.35	0.32	0.32
6-311G**	153.64	153.67	153.65	0.03	0.02	0.34	0.33	0.33
				MP2				
6-31G*	159.60	159.35	160.49	0.09	1.23	0.50	0.43	0.06
6-311G*	159.11	158.89	159.22	−0.22	0.11	0.26	0.37	0.37
6-311G**	158.64	158.64	158.72	0.00	0.07	0.36	0.32	0.32
				PCM				
B3LYP	157.90	157.19	157.24	−0.70	−0.66	0.14	0.45	0.41
MP2	157.61	157.59	157.61	0.02	0.00	0.33	0.34	0.33

parameters (G parameters) predicted an extremely weak band near 180 nm and blue-shifted the band around 205 nm. The poly-L-proline parameters (J parameters) showed the greatest sensitivity to chromophore placement; while the peak locations were typically comparable to those predicted using the original parameters, these parameters sometimes obtained inaccurate signs for the band around 180 nm. The α-helical parameters (H parameters) were also unable to reproduce the experimental CD spectra for any conformation. Although the peak locations predicted with the H parameters were relatively accurate, band signs were often incorrect.

For cyclo(L-Pro-L-Pro), a bandwidth of 3000 cm^{-1} provided the best agreement with experimental CD (Figures 4−7). The only exception was the CD from structures obtained by the CFF91 force field, which provided good qualitative accuracy using a 4000 cm^{-1} bandwidth. Although the 4000 cm^{-1} bandwidth is well-established as useful for describing experimental CD accurately,[2,32,39,73−75] the narrower band-fit peak of 3000 cm^{-1} may be necessary for taking into account the contribution of the higher-energy conformations (boat and chair) as the platter conformation consistently generates a very weak intensity CD spectrum, particularly in the negative band. All geometries resulted in negative band peak placement within 5 nm of the experimental value for individual conformations and weighted spectra. Peak intensities of the 185 nm band were closest to the experimental values for the MP2/6-311G**, BLYP 6-311G*, AMBER, and CFF91 DFT-weighted spectra (data available upon request).

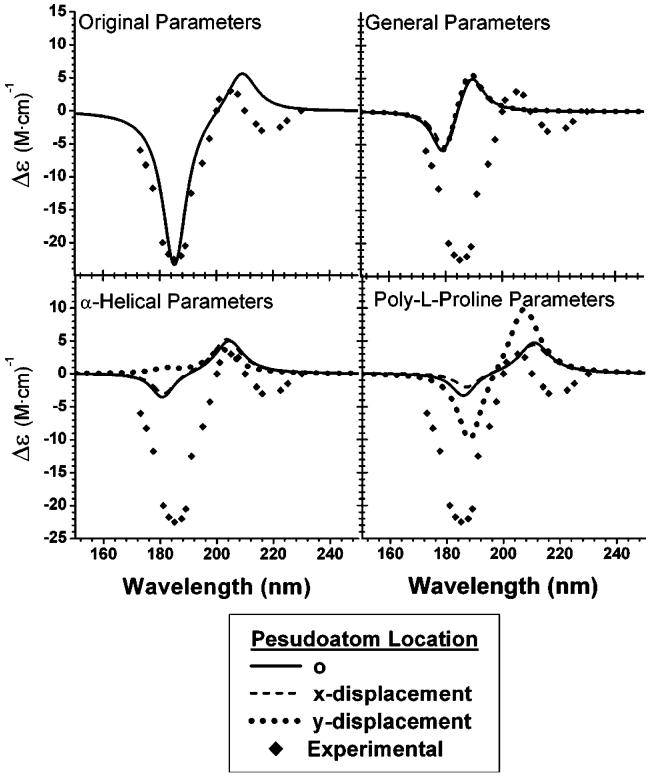

Figure 3. Comparison of different parameter set predictions for the CD spectra of cyclo(L-Pro-L-Pro) in the boat conformation. The peptide structure was optimized by the BVWN method using a 6-311G* basis set. Experimental CD obtained from Bowman et al.[4] The "o" position of the pseudoatom is halfway between the N and C′ atoms on the N—C′ bond. The "*x*" indicates a displacement of 0.1 Å toward the C′ atom from the "o" position. The "*y*" indicates a displacement of 0.1 Å into the N—C′—O plane from the "o" position. Bandwidth for each spectrum is 3000 cm^{-1}.

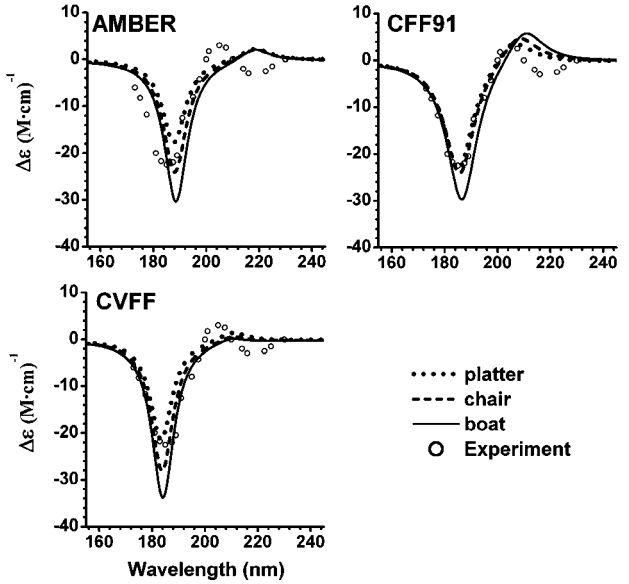

Figure 4. CD spectra of the three conformations of cyclo(L-Pro-L-Pro) as obtained by three molecular mechanics force fields in the gas phase. The original parameter set with bandwidth 3000 cm^{-1} is used for the AMBER and CVFF spectra, and the CFF91 spectra are calculated with a bandwidth of 4000 cm^{-1}. The experimental CD (in water) was obtained from Bowman et al.[4]

Discussion

Although there was some difficulty achieving reproducibility to all digits in energy convergence for each of the three conformations, it was comparatively easy to converge in individual calculations: repeated calculations yielded slightly differing energy values. For example, energies of the platter conformation as calculated using the BVWN method with a 6-311G** basis set varied by 5.4×10^{-3} kcal/mol depending on the initial structures (crystal vs built in InsightII from torsion angles). This indicates that cyclo(L-Pro-L-Pro) possesses a particularly flat potential energy. In general, structural determination for these molecules using DFT is comparable to MP2 in accuracy. Moreover, DFT methods required a significantly smaller basis set size than MP2 calculations to obtain good population distributions between the conformations.

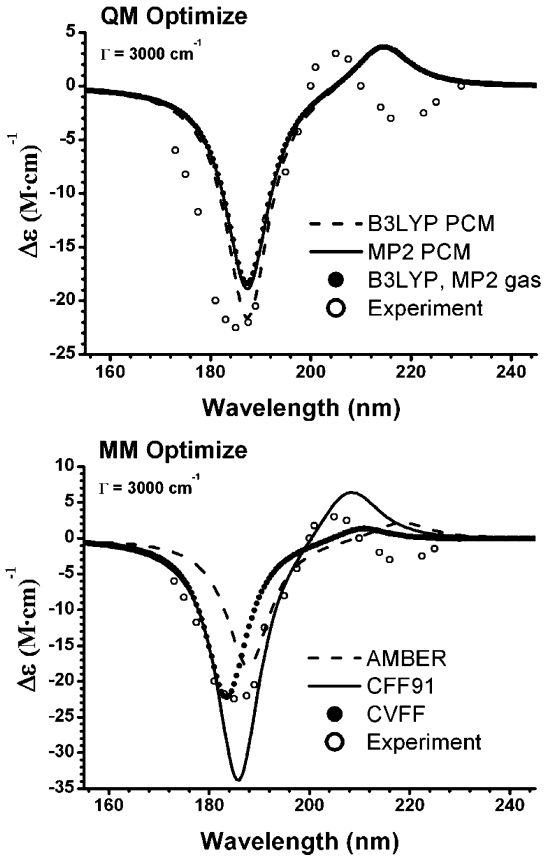

Figure 5. Boltzmann-weighted CD of QM and MM conformations in implicit water solvent. The energies used for weighting were obtained from the same method as the geometric optimizations.[5] The original parameter set with bandwidth of 3000 cm^{-1} is used for all calculations except CFF91 (4000 cm^{-1}). The experimental CD (in water) was obtained from Bowman et al.[4]

(1) Which Method of Structural Optimization is Best for Use with the Dipole Interaction Model for Cyclo(L-Pro-L-Pro)? The closest correspondence of band location and intensity with experimental CD was obtained by the CFF91, BLYP, and BVWN weighted CD spectra (Figures 5 and 7). The MP2 structures lead to theoretical CD that reflect the ratio of intensity of the two bands to each other well, but the second band is blue-shifted by over 10 nm, similar to the effect seen using RHF, B3LYP, and AMBER structures. Considering the poor ω (−14.2° to −17.3°) and ψ (41.6° to 56.0°) dihedral angle values of the CFF91 structures, the correspondence of the predicted CD using these structures to experimental values may be coincidental; the CFF91 results are particularly suspect, because MP2 calculations do not locate even local minimum-energy structures near those determined by CFF91. The structures yielding the best theoretical CD with the dipole interaction model are generated by MP2 and the pure DFT methods, but

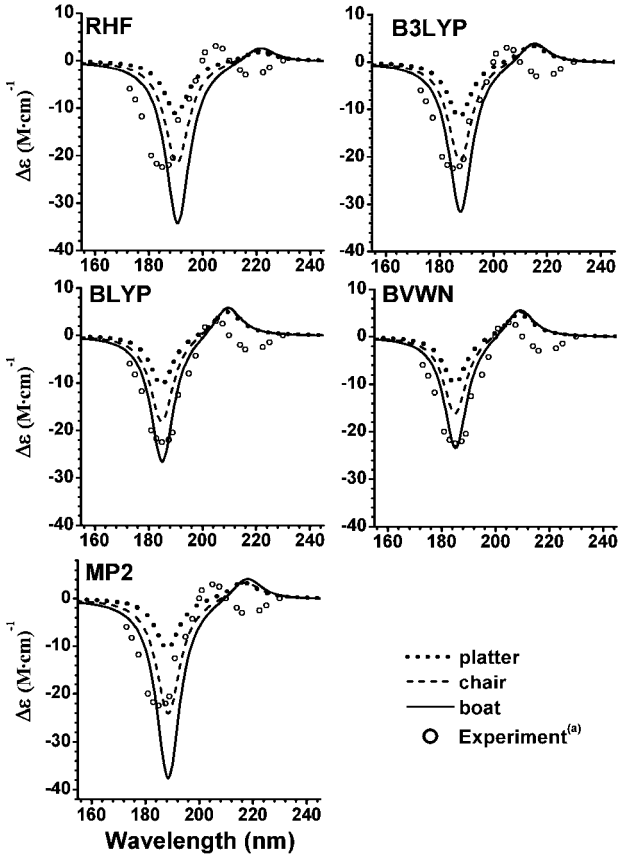

Figure 6. CD spectra of the three conformations of cyclo(L-Pro-L-Pro) as obtained by geometric optimization using quantum mechanics methods. The 6-311G* basis set was used for every optimization shown here except MP2, which used a 6-311G** basis set. The original parameter set with a bandwidth of 3000 cm^{-1} is used for each spectrum. The experimental CD (in water) was obtained from Bowman et al.[4]

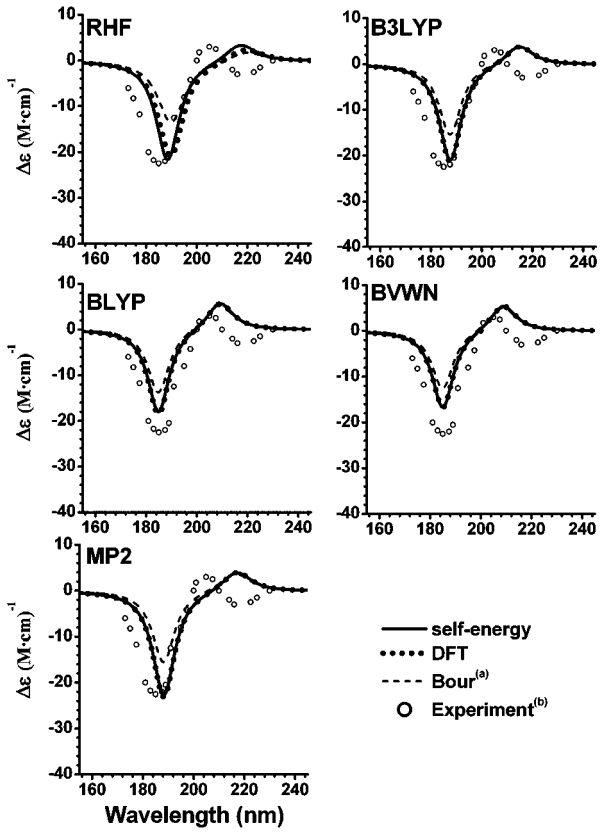

Figure 7. Boltzmann-weighted CD spectra of QM conformations of cyclo(L-Pro-L-Pro). The energies were obtained from (—) the same method as the geometric optimizations, (- - -) DFT/6-311G* energies, and (•••) the distribution suggested by Bour et al.[5] Geometric optimizations used the 6-311G* basis set, except for MP2, which used a 6-311G** basis. The original parameter set with a bandwidth of 3000 cm^{-1} is used for each spectrum. The experimental CD (in water) was obtained from Bowman et al.[4]

the DFT calculations required considerably smaller basis sets, consistent with our previous findings on other cyclic dipeptides.[1] Solvent effects were considered for DFT, MP2, and MM geometries. Inclusion of solvent terms via a dielectric constant for the molecular mechanics force fields had very little effect for either the AMBER or CVFF force fields (Figure 2), but CFF91 results exhibited considerable relaxation of $\phi-\psi$ strain. The B3LYP structure calculated with PCM was identical to that calculated by MP2 with PCM. The energy distribution was only minimally affected (Table 1), although it shifted the B3LYP calculations further toward preponderance of the boat and chair structures. Boltzmann-weighted spectra of both MP2 and B3LYP structures calculated with PCM were identical to the gas-weighted spectra (Figure 5). The PCM B3LYP structures led to CD with a more intense band at 190 nm than gas-phase B3LYP structures, causing this weighted spectrum to more closely resemble experiment. The minimial difference in overall spectrum and negligible effect on energy distribution, particularly in light of the different results of B3LYP and MP2 calculations, suggest that for this molecule, at least, inclusion of solvent effects in structural calculations is unnecessary.

(2) Which of the Dipole Interaction Parameters are Best Suited for Use for Cyclo(L-Pro-L-Pro), and Do They Coincide with the Optimal Parameters for Other Piperzaine-2,5-diones Studied Previously?[1] The original parameters performed best among the available dipole interaction model parameters for this cyclic dipeptide system, predicting peak location and peak sign qualitatively. This is consistent with our previous results concerning cyclic dipeptides.[1] As in our previous investigation of the CD of aliphatic piperazine-2,5-diones, the general parameters were both indistinguishable and nondescriptive of the experimental CD spectrum of cyclo(L-Pro-L-Pro). The α-helical and poly-L-Pro-II parameter sets generally predicted correctly the 180 nm band and a longer wavelength positive band, but were hypersensitive to chromophore placement and did not even qualitatively describe the relationship between the two $\pi-\pi^*$ bands. However, use of the original parameters resulted in the positive band being located at wavelengths longer than 215 nm for structures obtained by three methods (AMBER 218 nm, RHF 220 nm, MP2 216−218 nm); whereas the α-helical parameters located this band at much more realistic values (205−210 nm, all structures).

(3) How Quantitatively Do the Dipole Interaction Model's Predictions Compare with Experimental Values? The accuracy of the calculated CD spectra varies depending on which model geometries are used. The 185 nm band is located within 5 nm for all geometries, with the best overall location on the structures generated by the BVWN and BLYP (pure DFT) functionals. The depth of this band depended on the particular conformation, with the platter consistently having very low magnitude calculated values and the boat having the largest magnitude values for this band. The positive band, experimentally located at 205 nm, was consistently calculated by the dipole interaction model to center between 206 and 220 nm. The structures which led to the closest agreement of positive band location were CFF91 (206 nm) and both pure DFT functionals (BLYP, BVWN 209 nm).

The longer wavelength location of the positive band for many structures (B3LYP, 214 nm; MP2, 216 nm; AMBER, 218 nm) may be due to an underestimation of excitation energy from light perpendicular to the amide bonds in the original parameters. Additionally, the late appearance of this peak is likely influenced by noninclusion of the n−π* negative band peaking at 216 nm ($\Delta\epsilon = -3.0$) experimentally[4] in the dipole interaction model; inclusion of an n−π* transition would reduce the magnitude of the calculated positive band and shift its peak to shorter wavelengths. The broad width of the 205 nm band is then not particularly disturbing if the actual n−π* transition is stronger than would be suggested from a purely decoupled transition. Without inclusion of those parameters in this model, it is impossible to assess the contribution of n−π* band damping of the 205 nm $\pi-\pi$* band.

(4) Does the Dipole Interaction Model Recognize Poor Geometries (i.e., is it a good tool for evaluating molecular geometries)? CVFF and force field geometries of all three conformations possessed highly irregular ϕ and ψ values (Figure 2 and Supporting Information). The CD calculated using the dipole interaction model predicted a very weak, almost nonexistent positive band for these structures. The inclusion of solvent through a dielectric constant did not significantly improve either the dihedral angles (Figure 2 and Supporting Information) or the calculated CD (Figure 4) of the CVFF structures. The CFF91 structures yielded excellent theoretical CD (Figure 4) both in the gas phase and with the inclusion of water as solvent through a dielectric constant, with an improvement of predicted energies when the dielectric constant corresponding to solvation in water was used so that it resembled that of the MP2 calculations. It is possible that this agreement is coincidental, as the ω dihedral angles of the diketopiperazine rings obtained through the CFF91 force field minimizations are less planar than all other predictions and exceed the general guidelines of $\pm 15°$ for the amide bond twisting. Also, the ϕ torsions (Figure 2) for the platter conformation fall slightly outside the typical range of values for proline.[3] These geometries cannot be completely eliminated, however, because of the constrained nature of the ring system.

While red-shifted bands (and corresponding normal modes above 220 nm) have in the past been indicators of problems with structures,[3] it is likely that in this situation the shifting of the 205 nm band is a reflection of the dipole interaction model original parameters. These were developed assuming perfectly planar peptide bonds; an assumption which was used in the structural modeling of cyclo(L-Pro)$_2$ previously reported and potentially contributing to that study's apparent success at predicting the structure.[38] It is notable in the Sathyanarayana and Applequist study that side chain C−C bond lengths were chosen to be 1.54 Å. Our QM calculations agree with this value (data not shown), in disagreement with published crystal spectra (including the crystal structure used as basis for this study).[6,45,76] However, the bond angles and lengths chosen for that study did not correspond to any energy minimum and were instead selected as a "best fit". The strong influence of conformation on CD spectra for this cyclic dipeptide indicates that the excellent agreement of the spectra predicted by Sathyanarayana and Applequist may have been somewhat coincidental. It may also mean that intermediate conformations between the three minimum-energy ones play a considerable role in experimental CD, particularly if the molecule has a flat potential energy surface that allows it to convert between conformations rapidly.

(5) Can the Dipole Interaction Model Handle Multiple Conformations in a Shallow Potential Energy Surface? The three conformations of cyclo(L-Pro-L-Pro) generate CD spectra with differing ratios of band amplitudes for the $\pi-\pi$* transition at 185 and 205 nm (Supporting Information). The platter conformation possesses the lowest ratio of amplitudes of the three structures, regardless of method, while the boat conformation generated a very intense 185 nm band; the chair conformation was intermediate in this effect. The magnitude of the change for the 185 nm band with molecular conformation varied from 160% (CVFF) to 350% (MP2) relative to the platter-conformation depth for each trio of conformations. This strong sensitivity to the structure of the diketopiperazine ring is due to the differential alignment of the amide chromophore. In the platter conformation, the chromophore vectors are nearly horizontal to the plane of the molecule, whereas in the boat conformation, these vectors both have a significant perpendicular component. The perpendicular component is giving rise to the strong 185 nm band. While the intensity of the 185 nm band was quite sensitive to conformation, the intensity of the 205 nm band, dependent on the interaction with light parallel to the amide bond, was far less sensitive, experiencing a range of magnitude increases between platter and boat conformations between 110% (BLYP) and 165% (RHF). Thus, the model is able to distinguish between effects on spectra due to global conformation changes and those due to small geometric differences within one conformation.

The depth of the 185 nm band suggests that there must be significant population of the higher-energy (boat and chair) structures to reproduce the relative ratio of $\pi-\pi$* bands in the CD spectrum. All molecular mechanics methods predicted that, in the gas phase, the platter conformation is exclusive (Table 1). When solvent was included with a dielectric constant, energy calculations of only the CFF91 force field allowed for significant boat and chair contributions. Gas-phase RHF and MP2 energy calculations varied widely depending on the basis set used. The MP2/6-311G** calculations, however, suggest that the relative amounts of the three conformations are nearly equal, similar to all DFT calculations regardless of basis set size used here. Using CD to verify the presence of a conformation not confirmed by X-ray or NMR spectroscopy is not novel; a study with cyclo(Pro)$_3$ showed that a minor energy conformation was real and detectable via CD.[2] The agreement of our Boltzmann-weighted CD using this nearly equal distribution provides additional support to the energies obtained quantum mechanically that both the boat and the chair conformations exist in solution with greater representation than previously thought.[5] A thorough molecular dynamics study is needed to examine the nature of the potential energy surface and to observe how the dipole interaction model responds to molecular dynamics snapshots as opposed to assuming a thermal distribution in a Boltzmann ensemble.

Conclusions

The dipole interaction model qualitatively describes the $\pi-\pi$* transition feature of the UV CD spectra of cyclo(L-Pro-L-Pro) and approaches a quantitative prediction for the 185 nm band. All QM and one MM method generated set of structures lead to calculated CD in good agreement with experiment. The MP2 structure generated weighted CD were slightly more accurate than those calculated from pure DFT method structures with regard to peak location, depth of the 185 nm negative band, and relative depths of the two bands. However, the 205 nm band placement was shifted to higher wavelengths than can be accounted for solely by the missing n−π* transition for MP2-generated structures. This phenomenon appeared with the RHF and hybrid DFT structures as well. Pure DFT-generated

structures led to calculated CD with reasonable location of both peaks. Thus, when both CD bands were considered, pure DFT-calculated structures led to the best fit with experimental CD. Minimum-energy structures obtained by MP2 and DFT calculations suggest a nearly equal population of each of the three major conformations. Solvent effects, accounted for by use of implicit solvent via a dielectric constant with each molecular mechanics force field, did not affect the minimum-energy conformations, although the Boltzmann distribution obtained with the CFF91 force field shifted the balance toward the higher-energy boat and chair conformations, causing an improvement in calculated CD. Inclusion of solvent through PCM in the B3LYP and MP2 structural optimizations resulted in negligible structural differences, although the B3LYP distribution favored a larger population of chair and boat conformations. The weighted CD spectra obtained using MP2 structures calculated with PCM were indistinguishable from gas-phase calculations. The calculated CD of cyclo(L-Pro-L-Pro) suggests that all three minimum-energy conformations exist in significant amounts and may be rapidly interconverting in a shallow potential energy surface.

Acknowledgment. This work has been supported by the UND Seed Program, NIH ND BRIN and NIH grant no. P20 RR016741 from the INBRE Program of the National Center for Research Resources, and the North Dakota Computational Chemistry and Biology Network. K. Carlson has been supported by a Department of Education GAANN fellowship.

Supporting Information Available: Bond lengths, angles, and dihedral angles for each minimized structure. CD band analysis for each calculated CD using the gas-phase minimized structures. This material is available free of charge via the Internet at http://pubs.acs.org.

References and Notes

(1) Carlson, K. L.; Lowe, S. L.; Hoffmann, M. R.; Thomasson, K. A. *J. Phys. Chem A* **2005**, *109*, 5463.

(2) Lowe, S. L.; Pandey, R. R.; Czlapinski, J.; Kie-Adams, G.; Hoffmann, M. R.; Thomasson, K. A.; Pierce, K. S. *J. Pept. Res.* **2003**, *61*, 189.

(3) Thomasson, K. A. Proline side chain effects on theoretical $\pi-\pi^*$ absorption and circular dichroic spectra of proline-containing peptides. Doctoral Dissertation, Iowa State University, 1990.

(4) Bowman, R. L.; Kellerman, M.; Johnson, W. C., Jr. *Biopolymers* **1983**, *22*, 1045.

(5) Bour, P.; Sychrovsky, V.; Malon, P.; Hanzlikova, J.; Baumruk, V.; Pospisek, J.; Budesinsky, M. *J. Phys. Chem A* **2002**, *105*, 7321.

(6) Bendetti, E.; Goodman, M. *Cryst. Struct. Commun.* **1975**, *4*, 641.

(7) Sreerama, N.; Woody, R. W. *Protein Sci.* **2004**, *13*, 100.

(8) Sreerama, N.; Woody, R. W. *Anal. Biochem.* **2000**, *287*, 252.

(9) Sreerama, N.; Woody, R. W. Circular Dichroism of Peptides and Proteins. In *Circular Dichroism: Principles and Applications*; 2nd ed.; Berova, N., Nakanishi, K., Woody, R. W., Eds.; John Wiley & Sons: New York, 2000; p 601.

(10) Kelly, S. M.; Price, N. C. *Biochim. Biophys. Acta* **1997**, *1338*, 161.

(11) Osvath, S.; Gruebele, M. *Biophys. J.* **2003**, *85*, 1215.

(12) Chanez-Cardenas, M. E.; Fernandez-Velasco, D. A.; Vazquez-Contreras, E.; Coria, R.; Saab-Rincon, G.; Perez-Montfort, R. *Arch. Biochem. Biophys.* **2002**, *399*, 117.

(13) Greenfield, N. J.; Fowler, V. M. *Biophys. J.* **2002**, *82*, 2580.

(14) Tinoco, I., Jr. *Adv. Chem. Phys.* **1962**, *4*, 113.

(15) Bayley, P. M.; Nielsen, E. B.; Schellman, J. A. *J. Phys. Chem.* **1969**, *73*, 228.

(16) Woody, A.-Y. M.; Woody, R. W. *Biopolymers* **2003**, *72*, 500.

(17) Hirst, J. D.; Colella, K.; Gilbert, A. T. B. *J. Phys. Chem. B* **2003**, *107*, 11813.

(18) Sreerama, N.; Woody Robert, W. *Methods Enzymol.* **2004**, *383*, 318.

(19) Thomasson, K. A.; Applequist, J. *Biopolymers* **1991**, *31*, 529.

(20) Liu, Z.; Chen, K.; Ng, A.; Shi, Z.; Woody, R. W.; Kallenbach, N. R. *J. Am. Chem. Soc.* **2004**, *126*, 15141.

(21) Applequist, J.; Carl, J. R.; Fung, K.-K. *J. Am. Chem. Soc.* **1972**, *94*, 2952.

(22) Applequist, J.; Sundberg, K. R.; Olson, M. L.; Weiss, L. C. *J. Chem. Phys.* **1979**, *70*, 1240.

(23) Applequist, J.; Sundberg, K. R.; Olson, M. L.; Weiss, L. C. *J. Chem. Phys.* **1979**, *71*, 2330.

(24) Applequist, J. *J. Chem. Phys.* **1979**, *71*, 4332.

(25) Bode, K. A.; Applequist, J. *J. Phys. Chem.* **1996**, *100*, 17825.

(26) Applequist, J. *J. Chem. Phys.* **1979**, *71*, 4324.

(27) Applequist, J. *Biopolymers* **1981**, *20*, 387.

(28) Applequist, J. *J. Chem. Phys.* **1980**, *73*, 3521.

(29) Bode, K. A.; Applequist, J. *J. Phys. Chem.* **1996**, *100*, 17820.

(30) Bode, K. A.; Applequist, J. *J. Phys. Chem. A* **1997**, *101*, 9560.

(31) Applequist, J. *Biopolymers* **1982**, *21*, 779.

(32) Huber, A.; Nkabyo, E.; Warnok, R.; Skalsky, A.; Kuzel, M.; Gelling, V. J.; Dillman, T. B.; Ward, M. M.; Guo, R.; Kie-Adams, G.; Vollmer, S.; Ngassa, F. N.; Lowe, S. L.; Ouporov, I. V.; Thomasson, K. A. *J. Undergrad. Chem. Res.* **2003**, *2*, 145.

(33) Sathyanarayana, B. K.; Applequist, J. *Int. J. Pept. Protein Res.* **1986**, *27*, 86.

(34) Bode, K. A.; Applequist, J. *Biopolymers* **1997**, *42*, 855.

(35) Bode, K. A.; Applequist, J. *Macromolecules* **1997**, *30*, 2144.

(36) Applequist, J.; Bode, K. A. *J. Phys. Chem. A* **2000**, *104*, 7129.

(37) Applequist, J. *J. Phys. Chem. A* **2000**, *104*, 7133.

(38) Sathyanarayana, B. K.; Applequist, J. *Int. J. Pept. Protein Res.* **1985**, *26*, 518.

(39) McFarlane, K. J.; Humbert, M. M.; Thomasson, K. A. *Int. J. Pept. Protein Res.* **1996**, *47*, 447.

(40) Baumgartner, T.; Thomasson Kathryn, A. *Biophys. J.* **1996**, *70*, A104.

(41) Lowe, S. L.; Kadrmas, N.; Baumgartner, T.; Thomasson, K. A. Predicted Circular Dichroic Spectra of Cyclo(Pro-Gly)$_3$ by the Dipole Interaction Model Using Revised Parameters. North Dakota Academy of Science, 2000.

(42) Applequist, J. *Biopolymers* **1981**, *20*, 2311.

(43) Caldwell, J. W.; Applequist, J. *Biopolymers* **1984**, *23*, 1891.

(44) Bode, K. A.; Applequist, J. *J. Am. Chem. Soc.* **1998**, *120*, 10938.

(45) Sletten, E. *J. Am. Chem. Soc.* **1970**, *92*, 172.

(46) Bruno, I. J.; Cole, J. C.; Edgington, P. R.; Kessler, M.; Macrae, C. F.; McCabe, P.; Pearson, J.; Taylor, R. *Acta Crystallogr., Sect. B* **2002**, *58*, 389.

(47) Cornell, W. D.; Cieplak, P.; Bayly, C. I.; Gould, I. R.; Merz, K. M. J.; Ferguson, D. M.; Spellmeyer, D. C.; Fox, T.; Caldwell, J. W.; Kollman, P. A. *J. Am. Chem. Soc.* **1995**, *117*, 5179.

(48) Weiner, S. J.; Kollman, P. A.; Case, D. A.; Singh, U. C.; Ghio, C.; Alagona, G.; Profeta, S.; Weiner, P. *J. Am. Chem. Soc.* **1984**, *106*, 765.

(49) Dauber-Osguthorpe, P.; Roberts, V. A.; Osguthorpe, D. J.; Wolff, J.; Genest, M.; Hagler, A. T. *Proteins: Struct., Funct., Genet.* **1988**, *4*, 31.

(50) Schmidt, A. B.; Fine, R. M. *Mol. Simul.* **1994**, *13*, 347.

(51) Frisch, M. J.; Trucks, G. W.; Schlegel, H. B.; Scuseria, G. E.; Robb, M. A.; Cheeseman, J. R.; Zakrzewski, V. G.; Montgomery, J. A., Jr.; Stratmann, R. E.; Burant, J. C.; Dapprich, S.; Millam, J. M.; Daniels, A. D.; Kudin, K. N.; Strain, M. C.; Farkas, O.; Tomasi, J.; Barone, V.; Cossi, M.; Cammi, R.; Mennucci, B.; Pomelli, C.; Adamo, C.; Clifford, S.; Ochterski, J.; Petersson, G. A.; Ayala, P. Y.; Cui, Q.; Morokuma, K.; Malick, D. K.; Rabuck, A. D.; Raghavachari, K.; Foresman, J. B.; Cioslowski, J.; Ortiz, J. V.; Stefanov, B. B.; Liu, G.; Liashenko, A.; Piskorz, P.; Komaromi, I.; Gomperts, R.; Martin, R. L.; Fox, D. J.; Keith, T.; Al-Laham, M. A.; Peng, C. Y.; Nanayakkara, A.; Gonzalez, C.; Challacombe, M.; Gill, P. M. W.; Johnson, B. G.; Chen, W.; Wong, M. W.; Andres, J. L.; Head-Gordon, M.; Replogle, E. S.; Pople, J. A. *Gaussian 98*, revision A.11.4 ed.; Gaussian, Inc.: Pittsburgh, PA, 2002.

(52) Frisch, M. J.; Trucks, G. W.; Schlegel, H. B.; Scuseria, G. E.; Robb, M. A.; Cheeseman, J. R.; Montgomery, J., J. A.; Vreven, T.; Kudin, K. N.; Burant, J. C.; Millam, J. M.; Iyengar, S. S.; Tomasi, J.; Barone, V.; Mennucci, B.; Cossi, M.; Scalmani, G.; Rega, N.; Petersson, G. A.; Nakatsuji, H.; Hada, M.; Ehara, M.; Toyota, K.; Fukuda, R.; Hasegawa, J.; Ishida, M.; Nakajima, T.; Honda, Y.; Kitao, O.; Nakai, H.; Klene, M.; Li, X.; Knox, J. E.; Hratchian, H. P.; Cross, J. B.; Bakken, V.; Adamo, C.; Jaramillo, J.; Gomperts, R.; Stratmann, R. E.; Yazyev, O.; Austin, A. J.; Cammi, R.; Pomelli, C.; Ochterski, J. W.; Ayala, P. Y.; Morokuma, K.; Voth, G. A.; Salvador, P.; Dannenberg, J. J.; Zakrzewski, V. G.; Dapprich, S.; Daniels, A. D.; Strain, M. C.; Farkas, O.; Malick, D. K.; Rabuck, A. D.; Raghavachari, K.; Foresman, J. B.; Ortiz, J. V.; Cui, Q.; Baboul, A. G.; Clifford, S.; Cioslowski, J.; Stefanov, B. B.; Liu, G.; Liashenko, A.; Piskorz, P.; Komaromi, I.; Martin, R. L.; Fox, D. J.; Keith, T.; Al-Laham, M. A.; Peng, C. Y.; Nanayakkara, A.; Challacombe, M.; Gill, P. M. W.; Johnson, B.; Chen, W.; Wong, M. W.; Gonzalez, C.; Pople, J. A. *Gaussian 03*, revision C.02 ed.; Gaussian, Inc.: Wallingford CT, 2004.

(53) Becke, A. D. *Phys. Rev. A* **1988**, *38*, 3098.

(54) Lee, C.; Yang, W.; Parr, R. G. *Phys. Rev. B* **1988**, *37*, 785−789.

(55) Vosko, S. H.; Wilk, L.; Nusair, M. *Can. J. Phys.* **1980**, *58*, 1200.

(56) Miehlich, B.; Savin, A.; Stoll, H.; Preuss, H. *Chem. Phys. Lett.* **1989**, *157*, 200.

(57) Binkley, J. S.; Pople, J. A. *Int. J. Quantum Chem.* **1975**, *9*, 229.

(58) Møller, C.; Plesset, M. S. *Phys. Rev.* **1934**, *46*, 618.
(59) Binning, R. C., Jr.; Curtiss, L. A. *Int. J. Quantum Chem.* **1991**, *40*, 781.
(60) Ditchfield, R.; Hehre, W. J.; Pople, J. A. *J. Chem. Phys.* **1971**, *54*, 724.
(61) Wolf, G. C.; Hilton, C. W.; Prasad, C.; Miller, J.; Joseph, M.; Thorneycroft, I. H. *Am. J. Obst. Gyn.* **1990**, *162*, 740.
(62) Hariharan, P. C.; Pople, J. A. *Theor. Chim. Acta* **1973**, *28*, 213.
(63) Hariharan, P. C.; Pople, J. A. *Mol. Phys.* **1974**, *27*, 209.
(64) Hehre, W. J.; Ditchfield, R.; Pople, J. A. *J. Chem. Phys.* **1972**, *56*, 2257.
(65) Krishnan, R.; Binkley, J. S.; Seeger, R.; Pople, J. A. *J. Chem. Phys.* **1980**, *72*, 650.
(66) Cossi, M.; Scalmani, G.; Rega, N.; Barone, V. *J. Chem. Phys.* **2002**, *117*, 43.
(67) Cossi, M.; Barone, V.; Mennucci, B.; Tomasi, J. *Chem. Phys. Lett.* **1998**, *286*, 253.
(68) Mennucci, B.; Tomasi, J. *J. Chem. Phys.* **1997**, *106*, 5151.
(69) Cances, E.; Mennucci, B.; Tomasi, J. *J. Chem. Phys.* **1997**, *107*, 3032.
(70) Applequist, J. *Acc. Chem. Res.* **1977**, *10*, 79.
(71) Applequist, J. *J. Chem. Phys.* **1979**, *71*, 1983.
(72) Thomasson, K. A.; Applequist, J. *Biopolymers* **1990**, *30*, 437.
(73) Lii, J. H.; Allinger, N. L. *J. Comput. Chem.* **1991**, *12*, 186.
(74) Manning, M. C.; Woody, R. W. *Biopolymers* **1991**, *31*, 569.
(75) Jorgensen, W. L.; Tirado-Rives, J. *J. Am. Chem. Soc.* **1988**, *110*, 1657.
(76) Karle, I. L. *J. Am. Chem. Soc.* **1972**, *94*, 81.